

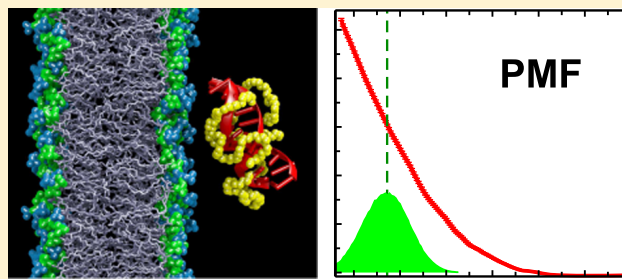
Molecular-Level Insight into the Interactions of DNA/Polycation Complexes with Model Cell Membranes

Andrey A. Gurtovenko*^{ID}

Institute of Macromolecular Compounds, Russian Academy of Sciences, Bolshoi Prospect V.O. 31, St. Petersburg 199004 Russia

Supporting Information

ABSTRACT: The interactions of DNA/polycation complexes (polyplexes) with cell membranes are crucial for understanding the molecular mechanisms behind polycation-mediated delivery of nucleic acid therapeutics into the target cells. In this study, we employed both biased and unbiased atomic-scale computer simulations to get an insight into such interactions. To this end, we considered complexes of DNA with linear polyethylenimine (PEI) with various polycation contents, ranging from an almost fully neutralized DNA to a highly overcharged polyplex. Our findings clearly show that the free energy gradually increases when a polyplex approaches the surface of a zwitterionic (neutral) phospholipid membrane from bulk water, implying the lack of attractive polyplex/membrane interactions. Remarkably, overcharging of DNA molecules by polycations enhances the repulsion between the polyplex and the zwitterionic lipid membrane. The observed repulsion is most likely driven by the dehydration of a polyplex upon its partitioning into the zwitterionic lipid membrane as well as by the loss of conformational entropy of PEI chains. We also demonstrate that cationic polymer chains are able to protect DNA from the dehydration as well as from contacts with lipid molecules. Interestingly, the absence of local minima in the free energy profiles does not exclude transient weak adsorption of a polyplex on the zwitterionic membrane surface. We show that such spontaneous adsorption can indeed be initiated by the interactions of loose polycation chains of the polyplex with polar head groups of lipids. Overall, our computational findings contribute considerably to the understanding of the initial stages in polycation-mediated DNA transfection. In particular, we demonstrate that a zwitterionic lipid bilayer represents an energetic barrier for polyplexes, so that a proper model of the cell membrane should account for the anionic surface charge of the membrane (e.g., due to the presence of proteoglycans).



INTRODUCTION

Basic concepts of gene therapy were first introduced almost five decades ago.¹ Recently, the progress in this research area has resulted in the appearance of first approved drugs on the market.² In general, the gene therapy relies on delivery of the genetic material into the target cells, this process being often assisted by certain vehicles (or delivery vectors) that are aimed to protect nucleic acids and to facilitate their translocation into the cells. Among numerous nonviral vectors for gene delivery,³ water-soluble cationic polymers are often considered as being exceptionally promising.⁴ This is in part due to the fact that the polycation's charge is opposite to the charge of polyanionic nucleic acids, so that the polymers are able to form compact electrostatically stabilized complexes with DNA/RNA molecules. Polycations used for gene delivery represent a very wide class of macromolecular compounds, ranging from natural cationic polymers (e.g., cationic chitosan, cationic cellulose, cationic dextran, and cyclodextrin) to their synthetic counterparts [e.g., poly-L-lysine, poly-L-arginine, polyethylenimine (PEI), and poly(amidoamine) dendrimers].^{4,5}

Besides the experimental efforts in this area, the use of polycations as delivery vectors of nucleic acids has also attracted a great deal of attention from computational

scientists.⁶ Computer simulations along with the models of high (atomistic) resolution are especially valuable in this context as they are able to complement experimental studies by providing a detailed, molecular-level insight into the interactions of polycations with DNA/RNA as well as the resulting complexes with cell membranes.

By far, most relevant computational studies have focused on the supramolecular complexes of DNA/siRNA with various cationic polymers. These include spermine,⁷ PEI,^{8–13} poly-L-lysine,^{8,11–17} poly-L-arginine,¹⁸ polyvinylamine,^{12,13} polyallylamine,^{12,13} supercharged pyridinium polycations,¹⁹ and ionenes.²⁰ Normally, computer simulations were used to follow the complexation of polycations with DNA/siRNA molecules and to explore the structure and binding patterns of the polycation/nucleic acid complexes (polyplexes).

While the formation of polyplexes is important, it represents only a preliminary step in the delivery process. Whichever pathway of cellular uptake takes place, at some point the complex “polycation/nucleic acid” comes in direct contact with

Received: May 29, 2019

Revised: July 8, 2019

Published: July 10, 2019

the cell membrane. Despite the obvious time- and length-scale limitations of atomistic computer simulations, such simulations are often the only means for extracting the microscopic information regarding the interactions of the polyplexes with membranes. Unfortunately, computational studies that go beyond the “polycation/DNA/RNA” complexes are still at a rudimentary level. In particular, Antipina and Gurtovenko recently published a series of computational studies that focused on the interactions of naked nucleic acids with model lipid membranes.^{21–23} They showed that in the absence of divalent cations (such as calcium) a polyanionic DNA molecule does not interact favorably with a zwitterionic phospholipid bilayer as evident from the corresponding free energy profile.²² Furthermore, Uludağ et al. employed steered molecular dynamics (MD) simulations to explore configurational changes in siRNA/PEI complexes upon their forced penetration through the phospholipid membrane.²⁴ The abovementioned papers are the only relevant computational studies in this area by far.

In this work, we make the next step toward understanding the polycation-mediated DNA delivery at an atomic scale and focus on the binding of polyplexes to the surface of the model cell membranes (zwitterionic phospholipid bilayers). To the best of our knowledge, this is the first study in which the polyplex/membrane binding is explored in detail. PEI was chosen as a cationic polymer in our study as it is often considered as one of the most efficient polymer agent for DNA delivery.^{25,26} Furthermore, PEI has extensively been studied both experimentally^{27,28} and computationally.^{8,9,11,12} We considered DNA/PEI complexes with various polycation contents (or N/P ratios), ranging from an almost fully neutralized DNA molecule to a highly overcharged polyplex. For all DNA/PEI complexes considered, we employed both biased and unbiased computer simulations to explore polyplex/membrane binding. We evaluated the free energy of binding of DNA/PEI complexes to the membranes as well as reported a putative mechanism of PEI-driven adsorption of a polyplex to the surface of a phospholipid membrane.

METHODS

We have performed atomic-scale MD simulations of complexes of a short fragment of double-stranded DNA with linear PEI chains. The complexes were placed nearby a palmitoyl-oleoyl-phosphatidylcholine (POPC) lipid membrane, such that a DNA fragment was parallel to the surface of the membrane, see Figure 1.

An extensively studied Dickerson’s dodecamer d-(CGCGAATTGCG)₂ (the total charge of $-22e$) was considered as a DNA fragment.^{29,30} A linear PEI chain consisted of 20 monomer units. The protonation level of PEI under physiological conditions^{31,32} was set to 50%, so that each PEI chain has the total charge of $+10e$. The number of PEI chains was varied from 2 to 4, leading to the N/P ratio in the complex (the ratio of the number of protonated amine groups of a polycation to that of DNA’s phosphate groups) equal to 20/22, 30/22, and 40/22, see Table 1. Initial configurations of the three DNA/PEI complexes were taken from ref 13. In turn, a lipid membrane consisted of 128 POPC molecules; its initial structure was taken from ref 22. Each DNA/PEI/bilayer system was solvated with $\sim 12\,000$ water molecules; counterions of both DNA (Na ions), and PEI (Cl ions) were added for electroneutrality. The total number of atoms in the systems under study amounted to $\sim 55\,000$.

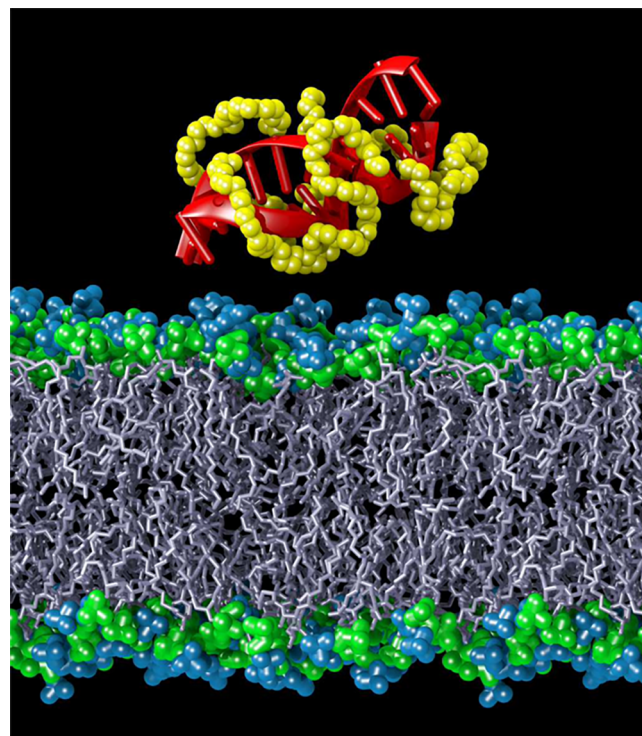


Figure 1. Snapshot of a DNA/PEI/membrane system. DNA is shown in red, PEI chains in yellow, choline, and phosphate groups of POPC lipids in blue and green, respectively; acyl chains of lipids are shown in ice blue.

Table 1. Simulated DNA/PEI/Bilayer Systems

system	# PEI chains	N/P ratio	simulation time [ns]
POPC-DNA-PEI2	2	20/22	35 \times 100
POPC-DNA-PEI3	3	30/22	35 \times 100
POPC-DNA-PEI4	4	40/22	35 \times 100
POPC-DNA ^a			35 \times 100
POPC-DNA-PEI2-des ^b	2	20/22	500
POPC-DNA-PEI3-des	3	30/22	500
POPC-DNA-PEI4-des	4	40/22	500
POPC-DNA-des			500
POPC-DNA-PEI2-ads ^c	2	20/22	10 \times 100
POPC-DNA-PEI3-ads	3	30/22	10 \times 100
POPC-DNA-PEI4-ads	4	40/22	10 \times 100

^aData taken from ref 22. ^bUnbiased simulations with the initial DNA/bilayer COM distance equal to 3 nm (“desorption” simulations).

^cUnbiased simulations with initial DNA/bilayer COM distances ranged from 3.9 to 4.8 nm (“adsorption” simulations).

The AMBER parmbsc0 set³³ of parameters was used to describe a DNA dodecamer, while the AMBER force-field Lipid14 was used for POPC lipids.³⁴ As far as PEI chains are concerned, we used an AMBER-compatible force-field developed previously.^{12,13,35} Water was represented by the TIP3P model.³⁶ Simulations were performed in the NPT ensemble at $T = 303$ K and $P = 1$ bar. Temperature and pressure were controlled with the use of the velocity-rescaling thermostat³⁷ and the Berendsen barostat,³⁸ respectively. The Lennard-Jones interactions were cutoff at 1 nm, while the long-ranged electrostatic interactions were handled with the use of the particle-mesh Ewald method.³⁹ The time step was set to 2 fs. The Gromacs 4.6.5 suite was used for simulations.⁴⁰

To evaluate the free energy of binding of a DNA/PEI complex to the surface of a POPC lipid bilayer, we used the umbrella sampling technique.⁴¹ A polyplex was placed in the vicinity of a lipid membrane. Because DNA/PEI complexes consisted of different numbers of PEI chains (see Table 1), we chose a distance between the centers of mass (COM) of a DNA dodecamer and a membrane in the direction perpendicular to the membrane surface to be a reaction coordinate. This ensures that the reaction coordinate does not depend on the polycation concentration. Starting configurations for umbrella sampling calculations were obtained by pulling the polyplex toward the membrane surface along the reaction coordinate. During pulling a velocity and a force constant were set to 0.025 nm/ps and 1000 kJ mol⁻¹ nm⁻², respectively. From the resulting trajectory, we extracted 35 windows with a spacing of 0.1 nm for umbrella sampling calculations (from 4.8 to 1.4 nm along the reaction coordinate). Each window was simulated for 100 ns with the force constant set to 3000 kJ mol⁻¹ nm⁻²; last 80 ns were used for subsequent free energy calculations. The Gromacs implementation⁴² of the weighted histogram analysis method⁴³ was used to calculate the potential of mean force (PMF). Statistical errors of the free energy were evaluated with the use of bootstrapping analysis.⁴² The accumulated simulation time of the biased simulations amounted to 10.5 μ s, see Table 1.

To get insight into the processes of desorption/adsorption of polyplexes from/on the surface of a lipid membrane, the PMF calculations were complemented by unbiased MD simulations. Overall, we performed two types of unbiased simulations. In the so-called “desorption” simulations, we considered a polyplex that was initially bound to the membrane surface (the initial distance between COMs of a DNA duplex and a lipid membrane was 3.0 nm). For each system, we performed a single 500 ns “desorption” simulation, see Table 1. In turn, the initial COM distance between a polyplex and a membrane in “adsorption” simulations was chosen in such a way that the polyplex was in the water phase in the vicinity of the membrane. For each nonzero PEI concentration, we performed 10 “adsorption” simulation runs (100 ns each) with different initial conditions. These conditions were varied by considering different initial DNA/membrane COM distances in the range from 3.9 to 4.8 nm (with a step of 0.1 nm), see Table 1. The initial configurations of the unbiased simulations were taken from the pulling trajectories (see above). The accumulated simulation time of the unbiased MD simulations was 5 μ s.

RESULTS AND DISCUSSION

Binding of Polyplexes to Lipid Membranes: Energetics. To explore the binding of DNA/PEI complexes to the model cell membranes, we employed biased MD simulations and calculated the free energy profile upon partitioning a polyplex from bulk water to the surface of a POPC lipid bilayer. The distance between COMs of a DNA molecule and a bilayer in the direction normal to the bilayer plane was chosen as a reaction coordinate. This way the free energy profiles for different polyplexes as well as for a naked DNA can be compared directly. In Figure 2, we present the corresponding free energy profiles (PMF) evaluated with the use of the umbrella sampling calculations.

Figure 2 clearly shows that all the free energy profiles for polyplexes have the same shape, this shape being similar to what was observed for a naked DNA (the POPC-DNA

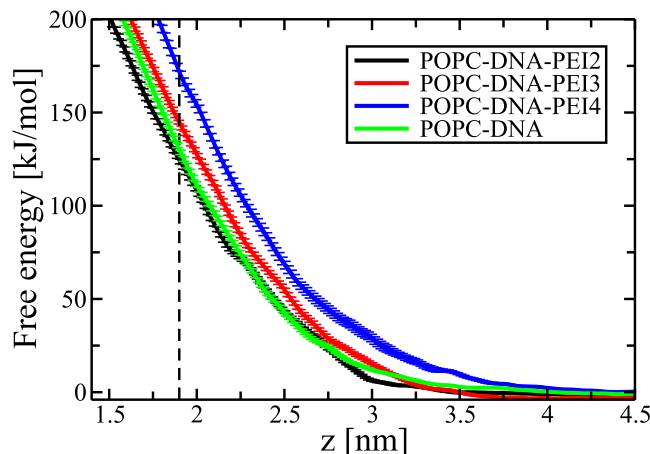


Figure 2. Free energy profile (PMF) for partitioning different DNA/PEI complexes (black, red and blues lines) and a naked DNA molecule (green line) from bulk water to the lipid/water interface of a POPC lipid bilayer along the reaction coordinate. A dashed line shows the average position of phosphate groups of POPC lipids.²² Statistical errors were estimated with the use of bootstrapping analysis.⁴²

system). As it was demonstrated in an earlier study,²² one can have a gradual growth of the free energy when a DNA molecule approaches the surface of a lipid bilayer from bulk water. Essentially, all polyplexes considered here show the same behavior: a steady increase of the free energy without any local minima upon approaching the bilayer surface from aqueous solution, implying the lack of attractive polyplex/lipid interactions. Therefore, we can conclude that cationic polymer chains do not reduce the energetic barrier for DNA binding to the surface of a zwitterionic lipid membrane.

Interestingly, the relative position of the free energy profiles for different polyplexes depends on the number of PEI chains in the polyplex. A PMF profile for the DNA/PEI complex with four polymer chains (the POPC-DNA-PEI4 system) deviates from zero already at a distance of 4 nm from the COM of the bilayer. This distance is noticeably larger than that observed for a naked DNA, see Figure 2. Similar behavior (although to a smaller extent) is also seen for the polyplex with three PEI chains. This can be explained by an overall positive charge of these polyplexes: +18e and +8e for the systems POPC-DNA-PEI4 and POPC-DNA-PEI3, respectively. This positive polyplex charge can lead to the electrostatic repulsive interactions between the polyplexes and choline groups of POPC lipids on the surface of the lipid bilayer. Therefore, overcharging of a DNA molecule by cationic polymer chains enhances the repulsion between the polyplex and the model lipid membrane.

It is also noteworthy that in contrast to polyplexes with 3 and 4 PEI chains, the free energy profiles for a naked DNA and an almost fully neutralized DNA (the POPC-DNA-PEI2 system with the overall charge of -2e) practically coincide, see Figure 2. While the polyplex with 2 PEI chains has a larger size as compared to a naked DNA, this difference in size seems to be compensated by its much smaller overall charge.

Close to the hydrocarbon core of a lipid bilayer, all PMF profiles demonstrate an abrupt growth of the free energy, which is something that can be expected for charged objects (polyplexes) in the hydrophobic environment. It is instructive to estimate the energetic cost for a polyplex to be embedded in

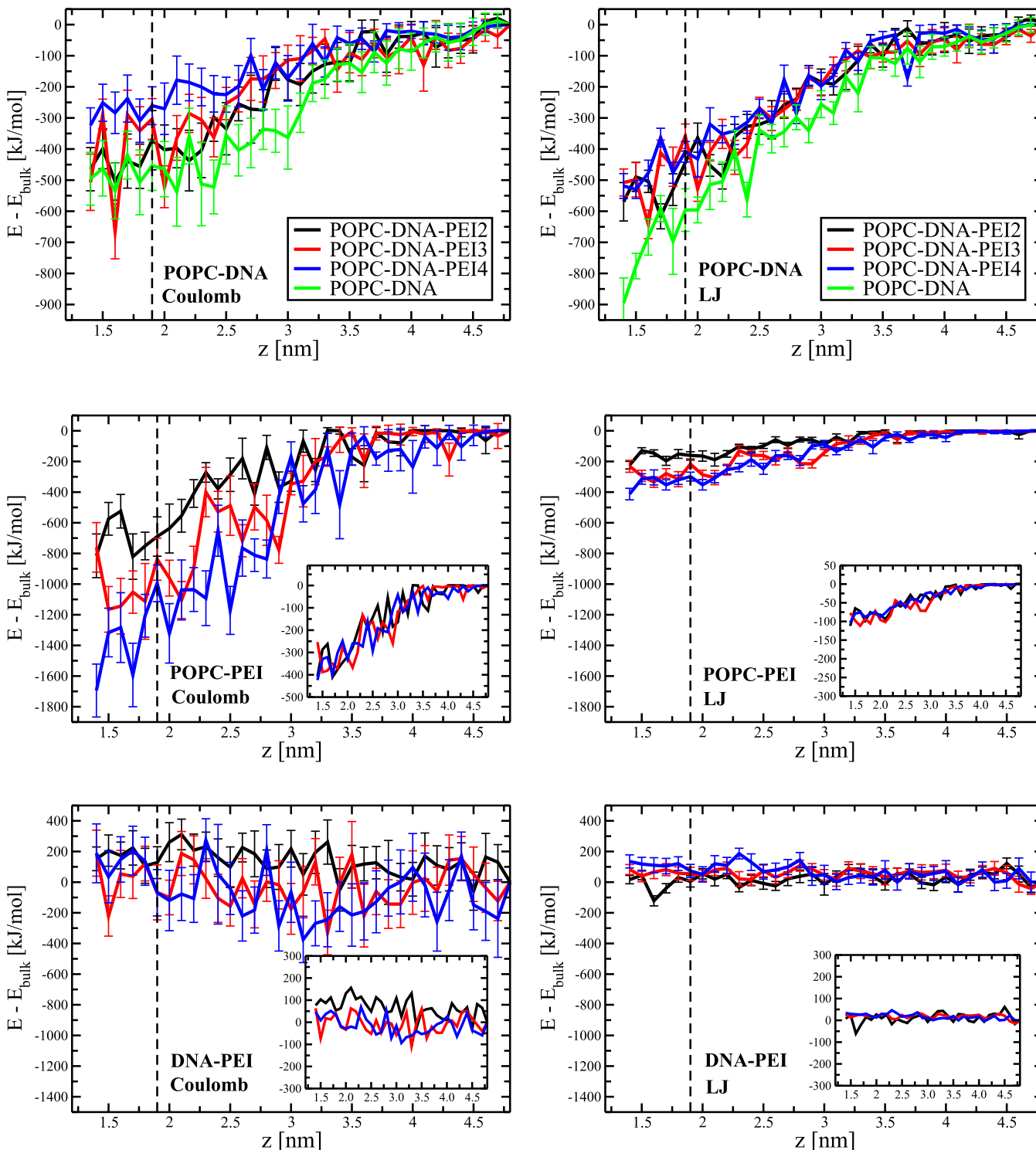


Figure 3. Changes in the nonbonded interaction energies as a function of the distance between COMs of a DNA and a lipid bilayer. Shown are the results for the POPC/DNA (top row), POPC/PEI (middle row), and DNA/PEI (bottom row) interactions. The insets show the energies per PEI chain. A dashed line indicates the average position of phosphate groups of POPC lipids.

the membrane as deep as the position of lipid phosphate groups (shown by a vertical dashed line in Figure 2). From Figure 2 one has 129, 124, 145, and 170 kJ/mol for POPC-DNA, POPC-DNA-PEI2, POPC-DNA-PEI3, and POPC-DNA-PEI4 systems, respectively. The energetic costs for POPC-DNA-PEI3 and POPC-DNA-PEI4 systems are noticeably larger than that for a naked DNA, which is again a sign of the elevated repulsion of cationic PEI chains and positively

charged choline groups of POPC lipids. Interestingly, a polyplex with two PEI chains and a naked DNA show very close values of free energy at the position of phosphate groups.

Besides the PMFs, it is also instructive to evaluate various components of the nonbonded energies (Coulomb and Lennard-Jones interactions) when a polyplex partitions into the lipid/bilayer interface during umbrella sampling calculations. In Figure 3, we present the changes of these energies

with respect to their values in bulk water for DNA/lipid, PEI/lipid, and DNA/PEI interactions. Remarkably, we found that both POPC/DNA and POPC/PEI interactions are favorable upon polyplex binding to the zwitterionic lipid membrane. Cationic polymer chains are found to effectively reduce the interactions between DNA and lipid molecules as seen for both Coulomb and Lennard-Jones energies, see Figure 3 (top row). The reduction in the energies implies the increase in the distance between lipid head groups and a DNA molecule: PEI chains cover the DNA surface and protect the DNA from close contacts with POPC lipids. This effect is more pronounced when the content of PEI chains increases in the polyplex. In turn, the PEI/lipid interactions are found to be attractive for all three types of polyplexes considered, see insets in Figure 3 (middle row). These interactions are obviously stronger when more PEI chains are involved. As far as DNA/PEI interactions within the polyplex are concerned, they tend to slightly weaken upon partition of a polyplex into the lipid membrane because of relatively strong POPC/DNA and POPC/PEI interactions, see Figure 3 (bottom row).

If the interactions of both DNA and PEI with lipids are attractive, what is the nature of the observed lack of attractive forces between the polyplex and the lipid membrane? To get insight into this, we calculated the number of hydrogen bonds of DNA and PEI chains with water molecules, see Figure 4. It turns out that partitioning of a polyplex into the lipid membrane is accompanied by a substantial loss of hydrogen bonds of DNA/PEI with water due to polyplex dehydration, which is energetically very unfavorable, see Figure S1. Interestingly, PEI chains are found to protect a DNA molecule from both the aqueous medium and the dehydration. In bulk water, a naked DNA forms a considerably larger number of hydrogen bonds compared to DNA/PEI complexes. Furthermore, the relative loss of hydrogen bonds between DNA and water molecules upon polyplex binding to the membrane decreases with the PEI content in the complex, see Figure 4 (top). In turn, the larger overall charge of cationic polymers in the system, the larger number of hydrogen bonds of PEI with water is broken upon polyplex binding. This effect seems to be additive as the number of broken hydrogen bonds per PEI chain is found to be almost the same for all polyplexes considered, see Figure 4 (bottom).

All the abovementioned conclusions are also supported by the consideration of the interaction energies of DNA and PEI with water, see Figure S1. What is more, combining the data presented in Figures 3 and S1 allows one to determine the major factors responsible for an increase in the free energy upon polyplex binding, see Figure 2. In Figure 5, we plot the total energy (both Coulomb and LJ contributions) calculated as a sum over the interaction energies of a polyplex with the lipid bilayer and water molecules. Remarkably, DNA/PEI- and PEI-free systems demonstrate pronouncedly different behavior. For a naked DNA (the POPC-DNA system), the DNA dehydration is the major factor of the observed repulsion between a DNA fragment and a lipid bilayer. In contrast, when PEI chains are present in the system, the polyplex dehydration cannot compensate for favorable DNA/POPC and PEI/POPC interactions, see Figure 5. Therefore, other factors can play a role such as the loss of conformational entropy of flexible PEI chains upon polyplex/membrane binding.

To get a detailed insight into the interactions of a polyplex with the lipid membrane upon partitioning, we calculated component-wise mass density profiles for DNA, PEI, POPC

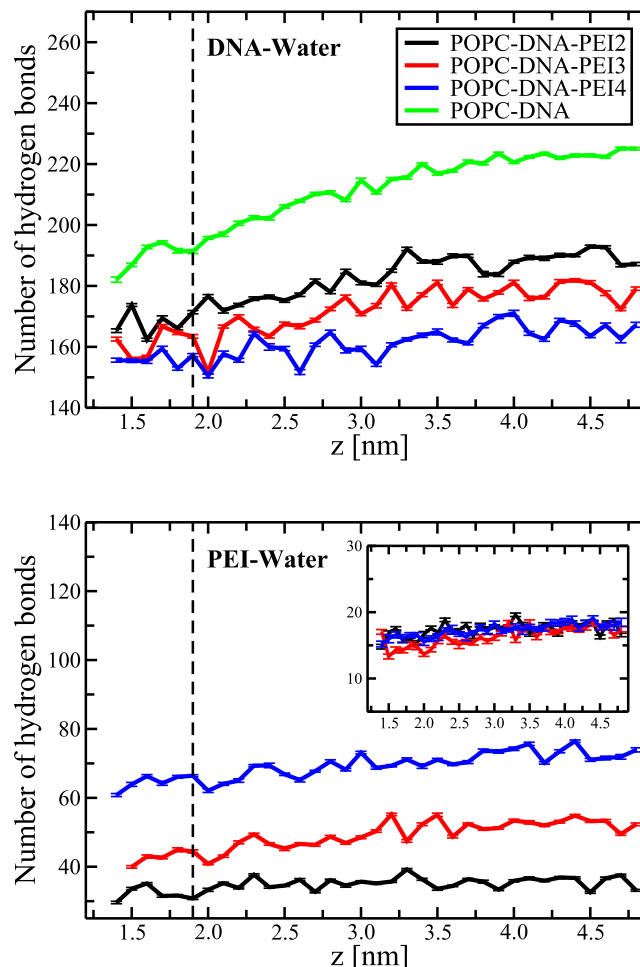


Figure 4. Number of hydrogen bonds of DNA (top) and PEI chains (bottom) with water molecules as a function of the distance between COMs of a DNA and a lipid bilayer. The inset shows the number of hydrogen bonds per PEI chain. A dashed line indicates the average position of phosphate groups of POPC lipids.

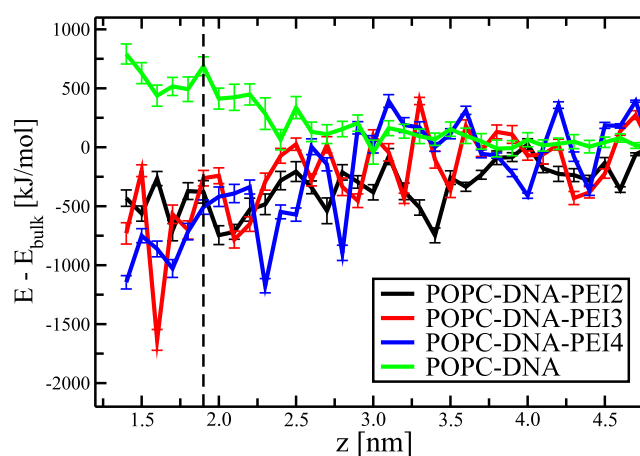


Figure 5. Changes in the nonbonded interaction energies as a function of the distance between COMs of a DNA and a lipid bilayer. Shown are the results for the total energy that accounts for the interactions of a polyplex with both the lipid bilayer and water molecules. A dashed line indicates the average position of phosphate groups of POPC lipids.

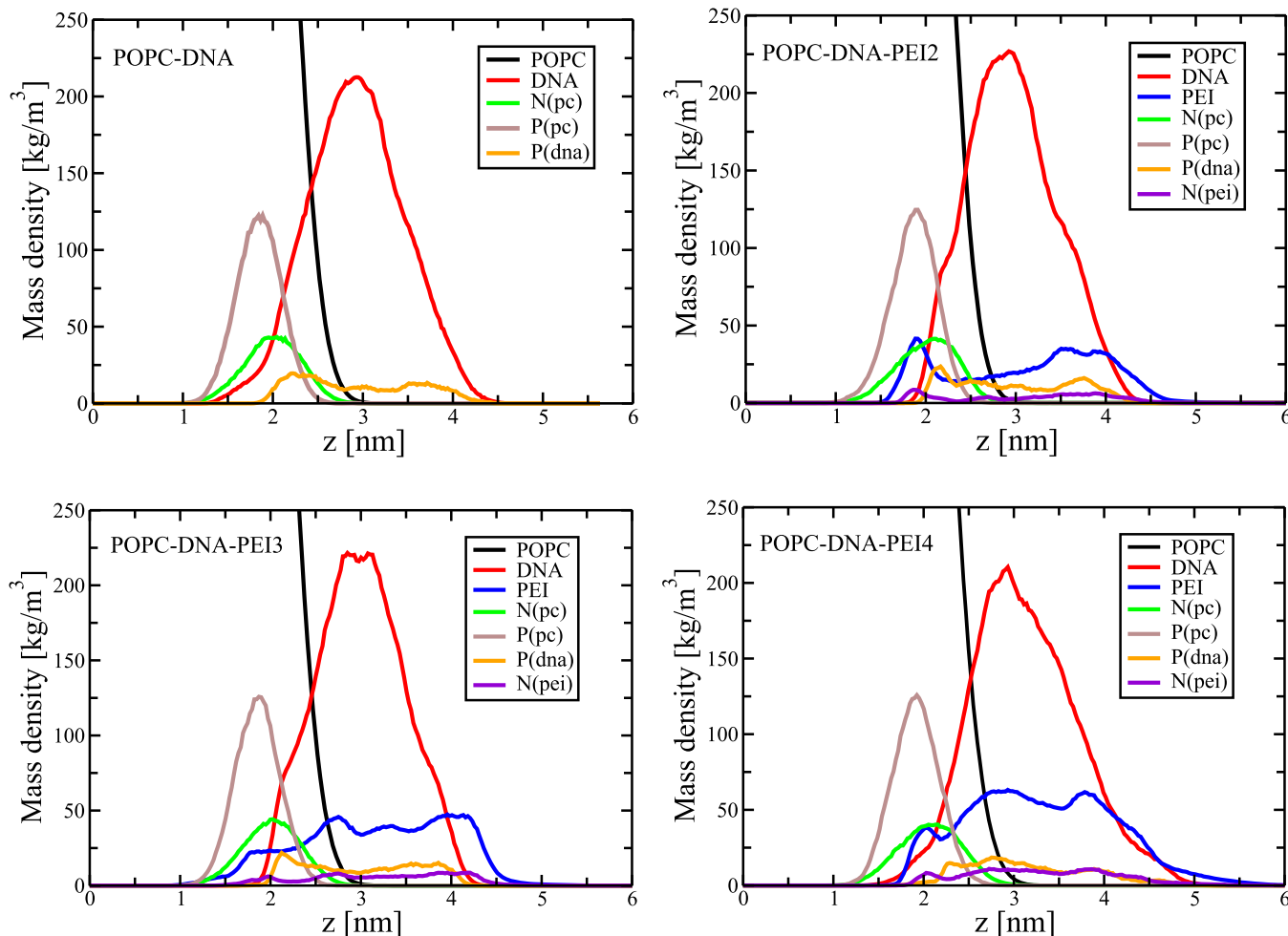


Figure 6. Component-wise mass density profiles for membrane/polyplex systems as a function of the distance from the membrane center (located at $z = 0$). Shown are the results for the PMF windows with the reaction coordinate equal to 3 nm, see Figure 2.

lipids, and their principal atoms (DNA's phosphate groups, PEI's protonated amine groups, and choline and phosphate groups of polar lipid head groups). For each system, we considered a PMF window at $z = 3.0$ nm, that is, the configuration at which a polyplex and a membrane has established a tight contact, see Figure 2. In Figure 6, we present the corresponding density profiles averaged over last 80 ns of 100 ns trajectories used for PMF calculations, see the Methods. Note that, while the COM distance between DNA and the membrane is fixed to 3.0 nm, the density profile for DNA is rather wide due to the fact that a DNA molecule can move on the membrane surface.

It is seen that the density profiles for phosphate groups of DNA demonstrate maxima that are localized close to the density profiles of choline groups of POPC lipids. This implies the attractive interactions between oppositely charged groups P(dna) and N(pc), see Figure 6. Such interactions were reported earlier for DNA/membrane systems in the situation when a DNA molecule adsorbs on the membrane surface due to divalent calcium cations.^{21,22} Here, a DNA fragment and a membrane are kept together by a harmonic potential used in umbrella sampling calculations. In turn, the density profiles of protonated amine groups of polymer chains develop peaks within the lipid/water interface close to the positions of lipid phosphate groups, see Figure 6. Therefore, one can conclude that favorable POPC/DNA (POPC/PEI) interactions in

Figure 3 are mainly driven by the interactions between choline groups and DNA's phosphate groups (phosphate groups of lipids and PEI's protonated amine groups).

Adsorption and Desorption of a Polyplex on/from Lipid Membranes. The absence of any local minima in the PMF profiles upon partitioning of a polyplex to a zwitterionic lipid bilayer implies that binding of DNA/PEI complexes to the surface of the bilayer is energetically unfavorable. However, this does not exclude a possibility of transient adsorption/desorption of a polyplex on/from the bilayer surface. In particular, there is no free energy barrier for DNA, reaching a distance of 3.5–4.0 nm from the COM of a POPC bilayer (see Figure 2), which could be sufficient for polyplex adsorption.

To get insight into such processes, we complemented our umbrella sampling calculations with two different sets of unbiased simulations. The starting configurations for both simulation sets were taken from PMF calculations. The first set (so-called “desorption” simulations) corresponds to the situation when a polyplex is initially in close contact with the surface of a lipid bilayer (the initial DNA/bilayer COM distance is equal to 3.0 nm). In turn, the second set (“adsorption” simulations) is based on the system configurations when a polyplex is in the water phase in the vicinity of the bilayer. Such “adsorption” simulations were repeated 10 times for each polyplex with different initial conditions (namely, with different initial DNA/membrane COM

distances ranged from 3.9 to 4.8 nm with a step of 0.1 nm), see Table 1.

In Figure 7, we plot the time evolution of the COM distance between DNA and a lipid bilayer when the polyplex is initially

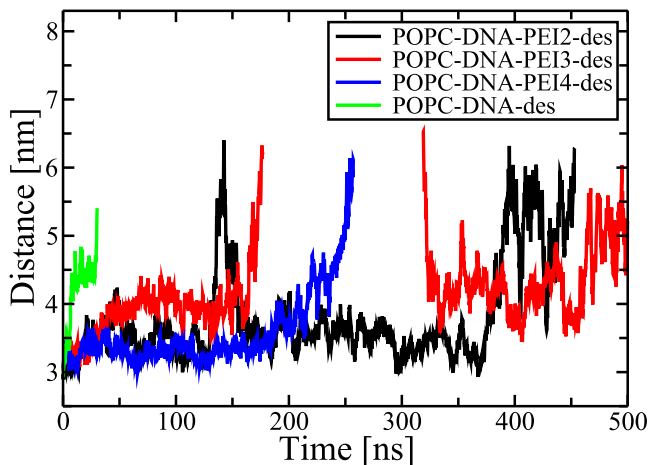


Figure 7. Distance between COMs of a DNA molecule and a lipid bilayer along the bilayer normal (z -axis) as a function of time.

attached to the bilayer (“desorption” simulations). First, one can see that in unbiased simulations, the polyplexes are able to remain adsorbed on the membrane surface for hundreds of nanoseconds. What is more, we found that the polyplexes can re-adsorb to the membrane surface after temporary desorption as seen for the POPC-DNA-PEI2-des system (at $t \approx 150$ ns) and the POPC-DNA-PEI3-des system (at $t \approx 300$ ns), see Figure 7. Note that, the gap in the distance curve for the POPC-DNA-PEI3-des system reflects the situation when the polyplex leaves the simulation box.

To explore a molecular mechanism behind adsorption/desorption of polyplexes, we calculated the number of contacts between DNA’s phosphate groups and lipid choline groups and also between protonated PEI amine groups and phosphate groups of POPC lipids, see Figure 8. First of all, it is seen that both these types of contacts (interactions) contribute to the binding of polyplexes to the membrane surface in line with the energy changes discussed in the previous section, see Figure 3. The relative contributions of DNA/POPC and PEI/POPC interactions obviously depend on the PEI content in the polyplex: the contacts of DNA with lipids are dominant for the polyplex with two PEI chains.

The most interesting feature in Figure 8 is the above-mentioned re-adsorption of a polyplex on the membrane surface, which is observed for the POPC-DNA-PEI2-des and POPC-DNA-PEI3-des systems. However, when considering adsorption of DNA/PEI complexes on the phospholipid membrane, special care has to be taken to exclude simulation artifacts. In particular, because of obvious limitations in time and length scales, in simulations, we consider only short fragments of DNA. Therefore, the nucleotides on both DNA ends are easily accessible for hydrogen binding with polar lipid groups. Such interactions emerge because of a finite size of a DNA molecule and should be treated as artifacts. This is in great contrast with siRNA molecules that are relatively short and can be simulated as a whole.²³ Turning now to re-adsorption of a polyplex to the membrane surface, Figure 8 (top) clearly shows the abovementioned artifacts related to a

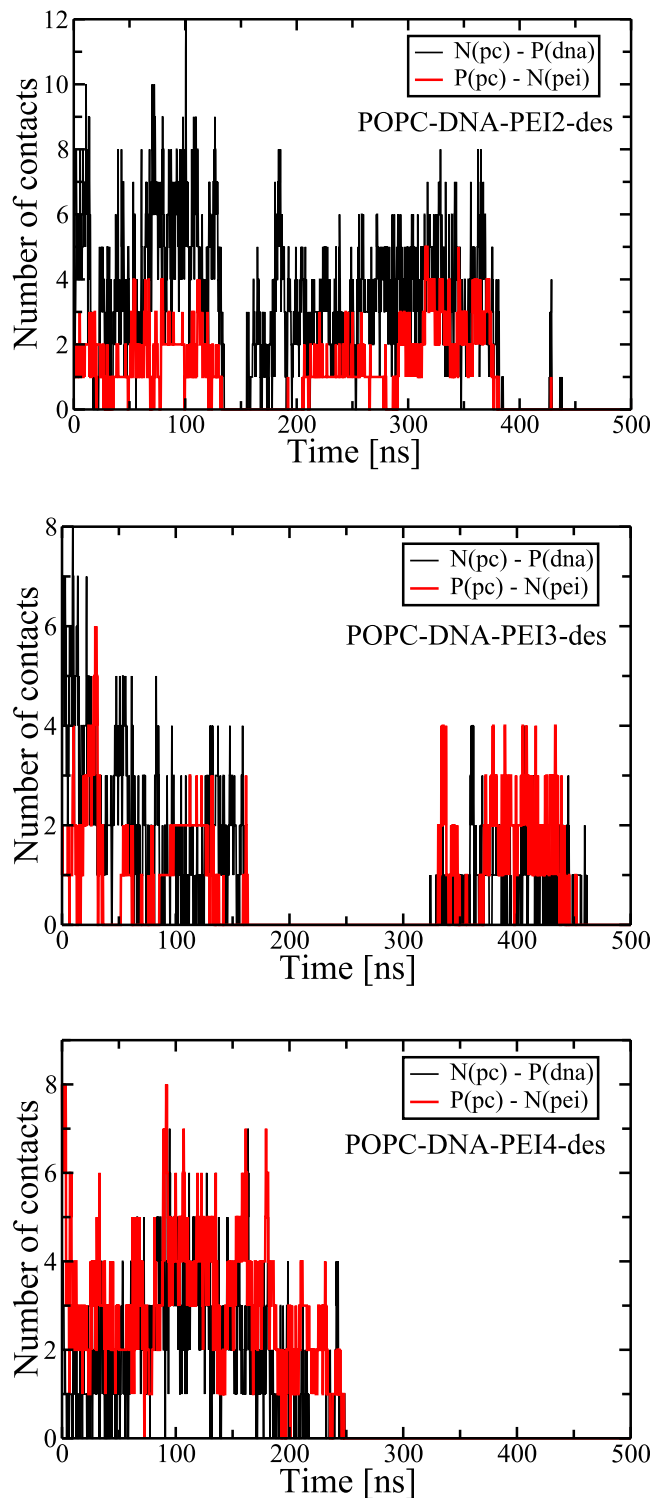


Figure 8. Number of contacts between DNA’s phosphate groups and lipid choline groups (black curves) and between protonated PEI amine groups and phosphate groups of lipids (red curves) as a function of time.

finite size of the DNA fragment at hand: the polyplex adsorption starts with establishing contacts between one of the DNA ends and polar lipid head groups at $t \approx 150$ ns, which are stabilized by PEI/POPC contacts 50 ns later.

On the other hand, the situation observed for the POPC/DNA/PEI3-des system [Figure 8 (middle) at $t \approx 330$ ns] is

much more relevant as the polyplex adsorption in this case is initiated by PEI chains that spontaneously attach to the lipid bilayer. This leads to binding of the polyplex to the bilayer surface as evidenced through formation of DNA/lipid contacts on a later stage. We emphasize that, this adsorption process is not associated with simulation artifacts because of DNA's finite size and can therefore be considered as a putative mechanism of polymer-induced adsorption of polyplex on the surface of a zwitterionic lipid membrane.

A typical sequence of events during the abovementioned PEI-induced adsorption is illustrated by a set of snapshots in Figure 9. The adsorption of a polyplex with 3 PEI chains,

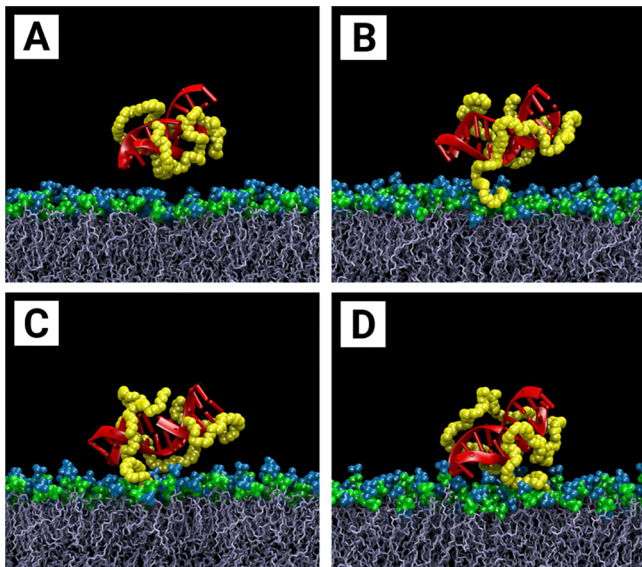


Figure 9. Polycation-induced adsorption of a DNA/PEI complex on the surface of a zwitterionic lipid membrane (the POPC-DNA-PEI3-des system): (A) 328.8, (B) 331.9, (C) 332.56, and (D) 336.64 ns. DNA is shown in red, PEI chains in yellow, and choline and phosphate groups of POPC lipids in blue and green, respectively. Acyl chains of POPC lipids are shown in ice blue.

which is initially located in the water phase (Figure 9A), starts with untwining of one of the PEI chains in the complex. This chain interacts with the membrane surface (Figure 9B), bringing the polyplex closer to the surface (Figure 9C). Eventually, the polyplex adsorbs on the lipid membrane, so that a DNA molecule establishes contacts with lipid polar head groups, see 9(D).

It has to be emphasized that the above conclusion regarding a possible molecular mechanism of the PEI-induced adsorption of a polyplex was based on just two instances of adsorption events that are seen in Figure 8. To make our conclusions more statistically reliable, for each polyplex, we performed 10 independent simulations (100 ns each) aiming to follow adsorption of a polyplex from water on the membrane surface, see Table 1. The time evolution of DNA/bilayer COM distances for all these 30 simulations is presented in Figure S2. Visual inspection of these plots indicates that the DNA/bilayer distances systematically shift to the larger values when the PEI content increases. This can be a signature of the elevated repulsion between a polyplex and lipid choline groups when the polyplex becomes more and more overcharged (i.e., more positively charged). Indeed, our analysis shows that out of 10 unbiased adsorption simulations, one has 9, 7, and 3

adsorption events for the POPC-DNA-PEI2-ads, POPC-DNA-PEI3-ads, and POPC-DNA-PEI4-ads systems, respectively. Importantly, we also observed 3 instances of the abovementioned PEI-induced adsorption (out of 30 simulations), supporting thereby the molecular mechanism presented in Figure 9.

CONCLUSIONS

The interactions of polyplexes with cell membranes are crucial for our understanding of the molecular mechanisms behind polycation-mediated delivery of nucleic acids into the target cells. In this study, we employed both biased and unbiased MD simulations to get a microscopic insight into such interactions. This allowed us to evaluate, for a first time, the free energy profiles for binding of polyplexes to the surface of a phospholipid membrane and explore possible mechanisms of polymer-induced polyplex adsorption.

Our findings clearly show that the free energy gradually increases when a polyplex approaches the surface of a zwitterionic phospholipid membrane from bulk water, implying the lack of attractive polyplex/lipid interactions. Analysis of various components of the nonbonded energies in the systems as well as hydrogen bonding indicates that this polyplex/membrane repulsion is most likely driven by the dehydration of a polyplex as well as by the loss of conformational entropy of PEI chains upon polyplex partitioning into the membrane. While the interactions of both DNA and polycations with lipid molecules are found to be attractive, the polyplex dehydration is accompanied by a considerable loss of hydrogen bonds between DNA/polycation with water molecules. Importantly, polycations are shown to protect a DNA molecule from dehydration, this effect being more pronounced at elevated polymer concentration. Furthermore, we found that cationic polymer chains, being part of a polyplex, effectively prevent the interactions between DNA and lipid molecules.

We also explored the role of polyplex overcharging and found that for overcharged polyplexes with a high positive charge, the polyplex/membrane repulsion is observed at larger distances from the membrane center as compared to almost fully neutralized DNA/polycation complexes as well as naked DNA. This effect is also confirmed by the results of unbiased adsorption simulations. Thus, overcharging of DNA molecules by cationic polymer chains enhances the repulsion between the polyplex and the zwitterionic lipid membrane.

The absence of local minima in the free energy profiles upon partitioning of polyplexes into the zwitterionic lipid membrane does not exclude transient adsorption of a polyplex on the membrane surface. Our unbiased simulations reveal that such transient polyplex adsorption indeed exists and can be initiated by the appearance of a loose polycation chain in the polyplex. The end of such a chain attaches to the membrane surface and eventually leads to the adsorption of the polyplex as a whole. We emphasize that such adsorption is reversible and rather weak.

To conclude, our atomic-scale computer simulations demonstrate that a zwitterionic phospholipid membrane represents a repulsive energetic barrier for a polyplex. In other words, cationic polymers do not facilitate interactions between a polyplex and a phospholipid membrane. This seems to contradict the general consensus that the overall cationic charge of a DNA/polycation complex enhances the transfection efficacy.⁴⁴ However, we recall that in our work, we

considered a zwitterionic (neutral) lipid bilayer as a model cell membrane. The use of a more realistic multicomponent membrane model should not change the overall picture as lipids in the outer leaflets of plasma membranes are mainly zwitterionic.⁴⁵ In reality, the plasma membrane has the negative surface charge due to the presence of anionic transmembrane proteoglycans.⁴⁶ Such anionic surface charge could promote the attractive interactions between polyplexes and the cell membranes and should be incorporated in future simulation studies.

■ ASSOCIATED CONTENT

S Supporting Information

The Supporting Information is available free of charge on the ACS Publications website at DOI: [10.1021/acs.jpcb.9b05110](https://doi.org/10.1021/acs.jpcb.9b05110).

Changes in the nonbonded energies for DNA/water and PEI/water interactions and time evolution of the DNA/bilayer distances in “adsorption” simulations ([PDF](#))

■ AUTHOR INFORMATION

Corresponding Author

*E-mail: a.gurtovenko@gmail.com. Phone: +7-812-3285601. Fax: +7-812-3286869. Web: biosimu.org.

ORCID

Andrey A. Gurtovenko: [0000-0002-9834-1617](https://orcid.org/0000-0002-9834-1617)

Notes

The author declares no competing financial interest.

■ ACKNOWLEDGMENTS

The author wishes to acknowledge the use of the computer cluster of the Institute of Macromolecular Compounds RAS and the Lomonosov supercomputer at the Moscow State University. This work was supported by the Russian Foundation of Basic Research through Grant 17-03-00446 and by the Presidium of the Russian Academy of Sciences through the grant program “Molecular and Cellular Biology”.

■ REFERENCES

- (1) Friedmann, T.; Roblin, R. Gene therapy for human genetic disease? *Science* **1972**, *175*, 949–955.
- (2) Dunbar, C. E.; High, K. A.; Joung, J. K.; Kohn, D. B.; Ozawa, K.; Sadelain, M. Gene therapy comes of age. *Science* **2018**, *359*, No. eaan4672.
- (3) Yin, H.; Kanasty, R. L.; Eltoukhy, A. A.; Vegas, A. J.; Dorkin, J. R.; Anderson, D. G. Non-viral vectors for gene-based therapy. *Nat. Rev. Genet.* **2014**, *15*, 541–555.
- (4) Lähelt, U.; Wagner, E. Nucleic acid therapeutics using polyplexes: A journey of 50 years (and beyond). *Chem. Rev.* **2015**, *115*, 11043–11078.
- (5) Samal, S. K.; Dash, M.; van Vlierberghe, S.; Kaplan, D. L.; Chiellini, E.; van Blitterswijk, C.; Moroni, L.; Dubrule, P. Cationic polymers and their therapeutic potential. *Chem. Soc. Rev.* **2012**, *41*, 7147–7194.
- (6) Meneksedag-Erol, D.; Tang, T.; Uludağ, H. Molecular modeling of polynucleotide complexes. *Biomaterials* **2014**, *35*, 7068–7076.
- (7) Korolev, N.; Lyubartsev, A. P.; Laaksonen, A.; Nordenskiöld, L. On the competition between water, sodium ions, and spermine in binding to DNA: a molecular dynamics computer simulation study. *Biophys. J.* **2002**, *82*, 2860–2875.
- (8) Ziebarth, J.; Wang, Y. Molecular dynamics simulations of DNA-polycation complex formation. *Biophys. J.* **2009**, *97*, 1971–1983.
- (9) Sun, C.; Tang, T.; Uludağ, H.; Cuervo, J. E. Molecular dynamics simulations of DNA/PEI complexes: Effect of PEI branching and protonation state. *Biophys. J.* **2011**, *100*, 2754–2763.
- (10) Sun, C.; Tang, T.; Uludağ, H. Molecular Dynamics Simulations for Complexation of DNA with 2 kDa PEI Reveal Profound Effect of PEI Architecture on Complexation. *J. Phys. Chem. B* **2012**, *116*, 2405–2413.
- (11) Antila, H. S.; Häkkinen, M.; Sammalkorpi, M. Chemistry specificity of DNA-polycation complex salt response: a simulation study of DNA, polylysine and polyethyleneimine. *Phys. Chem. Chem. Phys.* **2015**, *17*, 5279–5289.
- (12) Kondinskaia, D. A.; Kostritskii, A. Y.; Nesterenko, A. M.; Antipina, A. Y.; Gurtovenko, A. A. Atomic-scale molecular dynamics simulations of DNA-polycation complexes: Two distinct binding patterns. *J. Phys. Chem. B* **2016**, *120*, 6546–6554.
- (13) Kondinskaia, D. A.; Gurtovenko, A. A. Supramolecular complexes of DNA with cationic polymers: The effect of polymer concentration. *Polymer* **2018**, *142*, 277–284.
- (14) Ouyang, D.; Zhang, H.; Herten, D.-P.; Parekh, H. S.; Smith, S. C. Structure, Dynamics, and Energetics of siRNA–Cationic Vector Complexation: A Molecular Dynamics Study. *J. Phys. Chem. B* **2010**, *114*, 9220–9230.
- (15) Ouyang, D.; Zhang, H.; Parekh, H. S.; Smith, S. C. Structure and Dynamics of Multiple Cationic Vectors–siRNA Complexation by All-Atomic Molecular Dynamics Simulations. *J. Phys. Chem. B* **2010**, *114*, 9231–9237.
- (16) Elder, R. M.; Emrick, T.; Jayaraman, A. Understanding the effect of polylysine architecture on DNA binding using molecular dynamics simulations. *Biomacromolecules* **2011**, *12*, 3870–3879.
- (17) Antila, H. S.; Sammalkorpi, M. Polyelectrolyte decomplexation via addition of salt: Charge correlation driven zipper. *J. Phys. Chem. B* **2014**, *118*, 3226–3234.
- (18) Grasso, G.; Deriu, M. A.; Patrulea, V.; Borchard, G.; Möller, M.; Danani, A. Free energy landscape of siRNA-polycation complexation: Elucidating the effect of molecular geometry, polymer flexibility, and charge neutralization. *PLoS One* **2017**, *12*, No. e0186816.
- (19) Semenyuk, P. I.; Zhiryakova, M. V.; Izumrudov, V. A. Supercharged polyplexes: Full-atom molecular dynamics simulations and experimental study. *Macromolecules* **2018**, *51*, 5450–5459.
- (20) Seručník, M.; Podlipník, C.; Hribar-Lee, B. DNA-polyelectrolyte complexation study: The effect of polyion charge density and chemical nature of the counterions. *J. Phys. Chem. B* **2018**, *122*, 5381–5388.
- (21) Antipina, A. Y.; Gurtovenko, A. A. Molecular mechanism of calcium-induced adsorption of DNA on zwitterionic phospholipid membranes. *J. Phys. Chem. B* **2015**, *119*, 6638–6645.
- (22) Antipina, A. Y.; Gurtovenko, A. A. Molecular-level insight into the interactions of DNA with phospholipid bilayers: barriers and triggers. *RSC Adv.* **2016**, *6*, 36425–36432.
- (23) Antipina, A. Y.; Gurtovenko, A. A. Toward understanding liposome-based siRNA delivery vectors: Atomic-scale insight into siRNA-lipid interactions. *Langmuir* **2018**, *34*, 8685–8693.
- (24) Nademi, Y.; Tang, T.; Uludağ, H. Steered molecular dynamics simulations reveal a self-protecting configuration of nanoparticles during membrane penetration. *Nanoscale* **2018**, *10*, 17671–17682.
- (25) Luten, J.; van Nostrum, C. F.; De Smedt, S. C.; Hennink, W. E. Biodegradable polymers as non-viral carriers for plasmid DNA delivery. *J. Controlled Release* **2008**, *126*, 97–110.
- (26) Boussif, O.; Lezoualc'h, F.; Zanta, M. A.; Mergny, M. D.; Scherman, D.; Demeneix, B.; Behr, J. P. A versatile vector for gene and oligonucleotide transfer into cells in culture and in vivo: Polyethylenimine. *Proc. Natl. Acad. Sci. U.S.A.* **1995**, *92*, 7297–7301.
- (27) Godbey, W. T.; Wu, K. K.; Mikos, A. G. Poly(ethylenimine)-mediated gene delivery affects endothelial cell function and viability. *Biomaterials* **2001**, *22*, 471–480.
- (28) Tay, C. Y.; Menon, N.; Leong, D. T.; Tan, L. P. Molecular architecture governs cytotoxicity and gene transfection efficacy of polyethylenimine based nanoplexes in mammalian cell lines. *J. Inorg. Organomet. Polym.* **2015**, *25*, 301–311.
- (29) Drew, H. R.; Dickerson, R. E. Structure of a B-DNA dodecamer. *J. Mol. Biol.* **1981**, *151*, 535–556.

- (30) Dickerson, R. E.; Ng, H.-L. DNA structure from A to B. *Proc. Natl. Acad. Sci. U.S.A.* **2001**, *98*, 6986–6988.
- (31) Suh, J.; Paik, H. J.; Hwang, B. K. Ionization of Poly(ethylenimine) and Poly(allylamine) at Various pH's. *Bioorg. Chem.* **1994**, *22*, 318–327.
- (32) Smits, R. G.; Koper, G. J. M.; Mandel, M. The influence of nearest- and next-nearest-neighbor interactions on the potentiometric titration of linear poly(ethylenimine). *J. Phys. Chem.* **1993**, *97*, 5745–5751.
- (33) Pérez, A.; Marchán, I.; Svozil, D.; Sponer, J.; Cheatham, T. E.; Laughton, C. A.; Orozco, M. Refinement of the AMBER Force Field for Nucleic Acids: Improving the Description of α/γ Conformers. *Biophys. J.* **2007**, *92*, 3817–3829.
- (34) Dickson, C. J.; Madej, B. D.; Skjevik, Å. A.; Betz, R. M.; Teigen, K.; Gould, I. R.; Walker, R. C. Lipid14: The AMBER lipid force field. *J. Chem. Theory Comput.* **2014**, *10*, 865–879.
- (35) Kostritskii, A. Y.; Kondinskaia, D. A.; Nesterenko, A. M.; Gurtovenko, A. A. Adsorption of synthetic cationic polymers on model phospholipid membranes: Insight from atomic-scale molecular dynamics simulations. *Langmuir* **2016**, *32*, 10402–10414.
- (36) Jorgensen, W. L.; Chandrasekhar, J.; Madura, J. D.; Impey, R. W.; Klein, M. L. Comparison of simple potential functions for simulating liquid water. *J. Chem. Phys.* **1983**, *79*, 926–935.
- (37) Bussi, G.; Donadio, D.; Parrinello, M. Canonical sampling through velocity rescaling. *J. Chem. Phys.* **2007**, *126*, 014101.
- (38) Berendsen, H. J. C.; Postma, J. P. M.; van Gunsteren, W. F.; DiNola, A.; Haak, J. R. Molecular dynamics with coupling to an external bath. *J. Chem. Phys.* **1984**, *81*, 3684–3690.
- (39) Essmann, U.; Perera, L.; Berkowitz, M. L.; Darden, T.; Lee, H.; Pedersen, L. G. A smooth particle mesh Ewald method. *J. Chem. Phys.* **1995**, *103*, 8577–8593.
- (40) Hess, B.; Kutzner, C.; Van Der Spoel, D.; Lindahl, E. GROMACS 4: algorithms for highly efficient, load-balanced, and scalable molecular simulation. *J. Chem. Theory Comput.* **2008**, *4*, 435–447.
- (41) Torrie, G. M.; Valleau, J. P. Nonphysical sampling distributions in Monte Carlo free-energy estimation: Umbrella sampling. *J. Comput. Phys.* **1977**, *23*, 187–199.
- (42) Hub, J. S.; de Groot, B. L.; van der Spoel, D. g_wham-A Free Weighted Histogram Analysis Implementation Including Robust Error and Autocorrelation Estimates. *J. Chem. Theory Comput.* **2010**, *6*, 3713–3720.
- (43) Kumar, S.; Rosenberg, J. M.; Bouzida, D.; Swendsen, R. H.; Kollman, P. A. The Weighted Histogram Analysis Method for free-energy calculations on biomolecules. I. The method. *J. Comput. Chem.* **1992**, *13*, 1011–1021.
- (44) Hillaireau, H.; Couvreur, P. Nanocarriers' entry into the cell: relevance to drug delivery. *Cell. Mol. Life Sci.* **2009**, *66*, 2873–2896.
- (45) Gennis, R. B. *Biomembranes: Molecular Structure and Function*; Springer-Verlag: New York, 1989.
- (46) Neu, M.; Fischer, D.; Kissel, T. Recent advances in rational gene transfer vector design based on poly(ethylene imine) and its derivatives. *J. Gene Med.* **2005**, *7*, 992–1009.